Biochimica et Biophysica Acta 1850 (2015) 2304–2307

Contents lists available at ScienceDirect

Biochimica et Biophysica Acta

journal homepage: www.elsevier.com/locate/bbagen

Exogenous control over intracellular acidification: Enhancement via proton caged compounds coupled to gold nanoparticles

Marilena Carbone [a,b,*], Gianfranco Sabbatella [a,c], Simonetta Antonaroli [a], Hynd Remita [d], Viviana Orlando [e], Stefano Biagioni [e], Alessandro Nucara [f,g]

[a] Dept. of Chemical Sciences and Technologies, University of Rome Tor Vergata, Via della Ricerca Scientifica, 1-00133 Rome, Italy
[b] Consorzio Interuniversitario Biostrutture e Biosistemi, Viale Medaglie d'Oro 305, 00136 Rome, Italy
[c] Dept. of Chemistry, University of Rome La Sapienza, P.le A. Moro, 00185 Rome, Italy
[d] Laboratoire de Chimie Physique, UMR 8000-CNRS, Bât. 349, Université Paris-Sud, 91405 Orsay, France
[e] Dept. of Biology and Biotechnology "Charles Darwin", University of Rome La Sapienza, P.le A. Moro, 00185 Rome, Italy
[f] Dept. of Physics, University of Rome La Sapienza, P.le A. Moro, 00185 Rome, Italy
[g] Center for Life Nano Science, Istituto Italiano di Tecnologia, Viale Regina Elena 291, 00161 Rome, Italy

ARTICLE INFO

Article history:
Received 22 April 2015
Received in revised form 27 July 2015
Accepted 29 July 2015
Available online 31 July 2015

Keywords:
Proton caged compounds
Gold nanoparticles
pH monitoring
Intracellular acidification

ABSTRACT

The pH regulation has a fundamental role in several intracellular processes and its variation via exogenous compounds is a potential tool for intervening in the intracellular processes. Proton caged compounds (PPCs) release protons upon UV irradiation and may efficiently provoke intracellular on-command acidification. Here, we explore the intracellular pH variation, when purposely synthesized PCCs are coupled to gold nanoparticles (AuNPs) and dosed to HEK-293 cells. We detected the acidification process caused by the UV irradiation by monitoring the intensity of the asymmetric stretching mode of the CO_2 molecule at 2343 cm^{-1}.
The comparison between free and AuNPs functionalized proton caged compound demonstrates a highly enhanced CO_2 yield, hence pH variation, in the latter case. Finally, PCC functionalized AuNPs were marked with a purposely synthesized fluorescent marker and dosed to HEK-293 cells. The corresponding fluorescence optical images show green grains throughout the whole cytoplasm.

1. Introduction

Exogenous regulation of cellular functions has a fundamental role in medical treatments, such as cancer photodynamic therapy, where photosensitizers, typically porphyrins [1], phthalocyanines [2] and their derivatives are dosed or accumulated into cells and afterwards "turned on" via a selective photoexcitation [3]. The role of the photosensitizers is to transfer energy to tissue oxygen which undergoes a transition from triplet to singlet state and causes cellular apoptosis and necrosis [4,5]. Furthermore, it was shown that the association of photosensitizers with gold nanoparticles (AuNPs) enhances the photodynamic effect by improving the drug delivery [6,7].

Control over cellular functions may also be achieved through other fundamental parameters. Intracellular pH, for instance, plays a pivotal role in cellular processes and is highly regulated in every organelle [8]. The structural stability and function of proteins are tightly associated with the pH [9,10]. Osmotic response [11], ion transport [12] and membrane polarization [13] are pH-dependent. Furthermore, cell cycle progression and programmed cell death have both been linked to changes in intracellular pH [14,15]. Therefore, an exogenous control over the intracellular pH implies also a control over the related functions.

Caged compounds are light-sensitive probes bearing biomolecules in their inactive form. Upon irradiation, trapped molecules are liberated permitting targeted perturbation of a biological process [16].

It was recently shown that a photocontrolled acidification of the intracellular pH is possible, via a purposely synthesized photosensitive proton caged compound (PCC) [17]. In this study the 1-(2-nitrophenyl)-ethylhexadecyl sulfonate (HDNS) was dosed in 3T3-NIH fibroblasts and the cells irradiated in the UV-range (275–375 nm). The monitoring of the dosed cells by single-cell infrared spectromicroscopy showed an increase of the CO_2 asymmetric stretching vibration upon irradiation consequent to an intracellular acidification and subsequent decomposition of the H_2CO_3.

Following the previous study of intracellular acidification via exogenous compound, we probed the effects of associating AuNPs to photosensitive PCCs and monitored the intracellular effects upon irradiation. This required the synthesis of PPCs purposely functionalized with sulfur groups at one of the molecule ends, in order to bind to the AuNPs and form Self Assembled Monolayers.

To this purpose, a di-sulfided sulfonyl urethane compound, the disulfanediyldinonane-9,1-diylbis{[1-(2-nitrophenyl)ethoxy]sulfonyl} carbamate, which we named NESS-deca, was synthesized, characterized,

* Corresponding author at: Dept. of Chemical Sciences and Technologies, University of Rome Tor Vergata, Via della Ricerca Scientifica, 1-00133 Rome, Italy.

http://dx.doi.org/10.1016/j.bbagen.2015.07.011
0304-4165/

assembled with 22 nm diameter AuNPs and probed with respect to photoreactivity in the UV–vis range [18].

Here, we report on the effects of NESS-deca both free and bonded to AuNPs on intracellular pH of living HEK-293 cells, as a proof of principle. The studies were performed by infrared spectroscopy, since it allows non-destructive monitoring of the cells. Furthermore, the fingerprint of intracellular acidification is the increasing of CO_2 signal, which falls in a spectral region where typically cells have no vibrational structures.

For completion of the study, fluorescence images were taken of HEK-293 cells dosed with the NESS-deca functionalized AuNPs, which were previously marked with purposely synthesized fluorescent probes, to visualize the intracellular distribution of the functionalized AuNPs. Details on the synthesis of the fluorescent probe and characterization of the fluorescent probe, as well as the control experiments are reported in the Supplementary information.

Throughout the text the acronym NESS will be used for disulfide compounds, whereas NES indicated compounds where the disulfide bridge has been broken.

2. Materials and methods

2.1. Cell culture

Human embryonic kidney 293 (HEK-293) cells were grown in Dulbecco's Modified Eagle Medium (DMEM) supplemented with 2 mM glutamine, 10% FBS, maintained in a humidified incubator at 10% CO_2 and periodically tested to ensure the absence of mycoplasma contamination. Infrared spectroscopy observations were performed on cells cultured on UV-transparent CaF_2 windows, up to full coverage and incubated with 1 mg/mL PCCs. This corresponds to 2.4 mM free disulfided PCCs or 4.8 mM photogenerable H^+, and 0.046 mM photogenerable H^+ for the AuNPs–PCCs (PCCs are only 2% of the total weight of AuNPs–PCCs [18].

2.2. Infrared spectroscopy and photolysis

FTIR spectroscopy measurements were performed in transmission mode, with a Bruker IFS66/VS interferometer, under vacuum (~10^{-3} mbar), to avoid interference from atmospheric CO_2. The cells were housed in a sandwich holder and a 12 μm Mylar spacer was used to control sample thickness. UV radiation (275–375 nm) was provided by a deuterium discharge lamp (Acton Research Corporation) equipped with a band-pass (275–375 nm) FGUV11 filter (Thorlabs). The power density delivered to the sample is of the order of 0.1 W/mm^2.

In photolysis experiment, an area of ca 7 mm^2 was illuminated by UV-light. FTIR spectra have been collected with a spectral resolution of 2 cm^{-1}.

The cells were monitored for a few minutes by acquiring sequential FTIR spectra in the dark. After confirming stability of the spectra, measurements were interrupted and the cells were irradiated for 1 min with near-UV light. FTIR measurements were resumed after the illumination period and repeated at least thirty times before a subsequent illumination. All experiments, including controls, were done in duplicate.

2.3. Fluorescence imaging

Images of AuNP-NES-deca marked with nonyl-disulfide-fluoresceinisothiocyanate, a purposely synthesized fluorescent probe, were taken using an ApoTome System (Zeiss) connected with an AxioObserver Z1 inverted microscope (Zeiss). Nuclei of the cells were labeled with DAPI after the dosing of the marked AuNP-NES-deca. Cells were fixed in 4% paraformaldehyde for 15 min and then three times washed with PBS.

The synthesis and characterization of nonyl-disulfide-fluoresceinisothiocyanate, additional details of cell growth, FTIR measurements and control experiments are reported in the Supplementary information.

3. Results and discussion

In a previous study it was shown that a proton caged compound, the HDNS, may induce intracellular acidification, upon near-UV irradiation [17]. Here, we were interested in probing the joint effects of PCCs associated to AuNPs, as a proof-of-principle. Therefore, a new compound had to be synthesized which bears the proton caging functionality on one end and a sulfur containing moiety to bind AuNPs on the other end. NESS-deca (Sketch 1, which has in common with HDNS the o-nitrobenzoic ester chromophore, sensitive to illumination in the near-UV spectral region) was therefore synthesized. The alkyl chain in NESS-deca is shorter than in the HDNS and its photoreactivity, both free and bonded with AuNPs, was verified [18].

We incubated the CaF_2 windows full-coated with HEK-293 cells with either free or AuNP-functionalized NES-deca and, after photolysis, cellular acidification was followed by measuring changes in the intensity of the absorption band at 2343 cm^{-1}, formally assigned as the ν^3 fundamental vibration of aqueous CO_2 (CO_2(aq)) [19]. This band which has the advantage of appearing in a fairly clear region of the IR spectrum, is sharp and is easily resolved from most other absorption bands.

In Fig. 1a) and b), the infrared absorption spectra of the HEK-293 cells dosed with either free or functionalized NESS-deca upon photolysis pulses are reported in the spectral region 2300–2400 cm^{-1}. The spectra are normalized by the first spectrum after irradiation and by the initial concentration of photogenerable protons. Fig. 1 shows that the irradiation of cells dosed with NESS-deca free and functionalized with AuNPs causes an increase of the CO_2, though there is a marked difference of CO_2 yield in the two cases, the latter being ~400 times more intense. The peak area of the CO_2 band as a function of time is plotted in Fig. 2a) and b) and fitted with lines. The fitting parameters are: Fig. 2a) slope = $(2.38 \pm 0.05) * 10^{-5}$, intercept = $(7.47 \pm 0.1) * 10^{-3}$, Fig. 2b) slope = $(1.46 \pm 0.03) * 10^{-6}$, intercept = $(1.07 \pm 0.01) * 10^{-3}$. The data reproducibility from the 100% line is 0.5% ÷ 1%. The signal-to-noise ratio in the 2300–2400 cm^{-1} range is reported in the inset of Fig. 2b).

In order to rule out that the effects observed were related to intrinsic intracellular phenomena triggered by the irradiation, or due to traces of leftover compounds in the medium, control measurements were performed. Each of the compounds in DMEM solution as well as a sample of untreated cells maintained in DMEM, and one cell dosed with 1 mg/mL AuNPs were irradiated by UV and monitored by infrared in the same spectral region. In all cases the spectra in the 2300–2400 cm^{-1} are structureless, as reported in Fig. 1S in the Supplementary Information.

Finally, the NES-deca-AuNPs were marked with a purposely synthesized fluorescent probe (SS-nonyl-FITC, see the Supplementary information for synthesis details) and dosed to HEK-293 cells cultured onto CaF_2 windows. The images of dosed cells are reported in Fig. 3 in bright

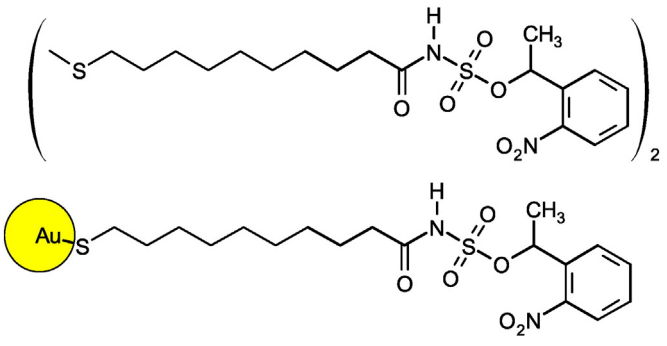

Sketch 1. NESS-deca and NES-deca functionalized with AuNPs.

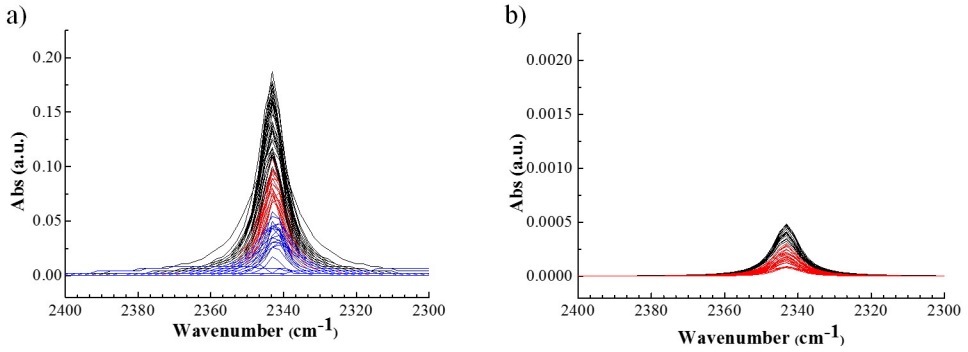

Fig. 1. CO_2 absorption band after irradiation of dosed HEK-293 cells; a) cells dosed with NESS-deca-AuNPs, b) cells dosed with free NESS-deca. Different colors refer to different irradiation rounds. Note that the scale of the left panel is 100 times larger than the scale of right one.

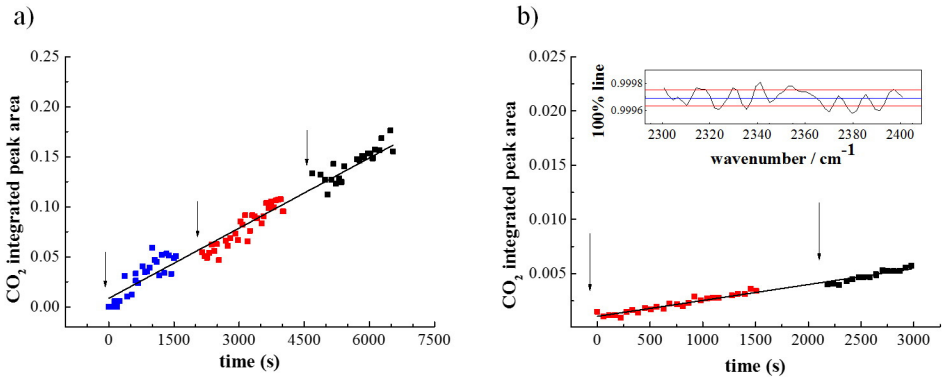

Fig. 2. Integrated peak area of CO_2absorption as a function of time: a) cells dosed with NES-deca-AuNPs, b) cells dosed with free NESS-deca. The arrows indicate the irradiation events. Different colors refer to different irradiation rounds. Note, also in this figure, the difference of scale between the two panels. The inset in panel b) is the signal-to-noise ratio.

field and in fluorescence. It can be seen that small green fluorescent grains are distributed throughout the whole cytoplasm.

The strong enhancement of the CO_2 yield when cells, dosed with NES-deca coupled with AuNPs, were irradiated may have different causes, though difficult to disentangle from each other: *i*) larger intracellular concentration of photogenerable protons and *ii*) more localized generation of protons. AuNPs have vectorial properties and are often employed as nanocarriers of compounds inside cellular media [20]. This mechanism may apply to our case too, enhancing the intracellular concentration of PCCs with respect to the dosing of free compound.

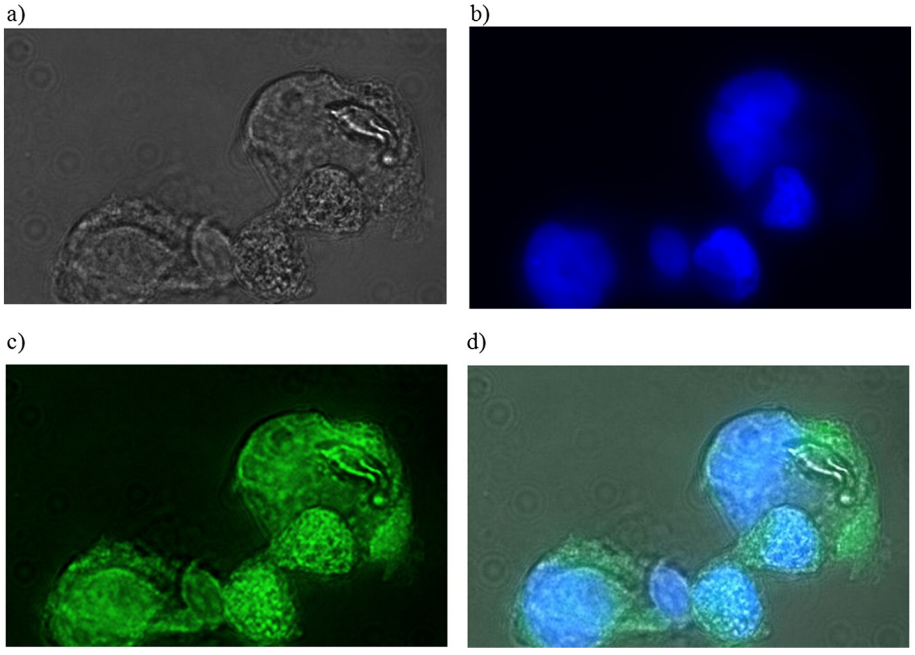

Fig. 3. Images of the HEK-293 cells dosed with NES-deca-AuNPs, marked with SS-nonyl-FITC. Magnification 40×. a) Bright field, b) blue light fluorescence of the nuclei labeled with DAPI, c) green light fluorescence, d) merged fluorescence in the blue, green and red light regions.

When PCCs are bonded to AuNPs they are forced to be localized around the particles. This implies a localized proton release around the particles upon irradiation. As a consequence, the acidification process is more inhomogeneous compared to the free PCCs. It can be envisaged that strong localized pH variations are more difficult to buffer by the intrinsic intracellular mechanisms [21], with net stronger acidification.

The monotonous increase of the CO_2 after the first irradiation is different from the observations in single-cell experiments, where the CO_2 production abruptly increased after each irradiation event. A few differences between the two experiments must be mentioned: the cells employed are different (HEK-293 vs 3T3-NIH) as well as the coverage of the window, nearly 100% in the present paper vs 20%–30% in the single cell experiment and the irradiated area, which is ca 7 mm^2 in the current study and the area of a single cell in the previous paper. A simple explanation for the different behaviors is that, in the current case, the first irradiation is sufficient to uncage all protons of the PCCs, and what we actually observe is a kinetic effect, i.e. a sort uncaging delay, which causes protons not to be released all simultaneously. An alternative explanation is a cooperative effect of neighboring cells when they simultaneously undergo an acidification process, which progressively deactivates the intrinsic buffer mechanisms.

In both cases, the effect is more pronounced when PCCs are bonded to AuNPs, as the slope of the CO_2 band integral increases more steadily as compared to free PCCs.

4. Conclusions

In this paper we probed the effects of coupling AuNPs to a purposely synthesized PCC, the NESS-deca, on intracellular acidification. Both free NESS-deca and NES-deca-AuNPs were dosed to HEK-293 fully covering CaF_2 windows. The acidification was triggered by UV irradiation and probed by infrared spectroscopy. The protons released upon irradiation bind intracellular HCO_3 to yield H_2CO_3 which decomposes in H_2O and CO_2, with a characteristic fingerprint at 2343 cm^{-1}.

We found out that AuNPs strongly enhance the intracellular acidification process, i.e. by a factor of nearly 400. This effect may be related both to an increased intracellular concentration of the exogenous agent, due to the vectorization via AuNPs, as well as to decreased efficiency of the buffer mechanism especially with more localized proton generation.

The CO_2 yield increases monotonously after the first irradiation event.

Finally, the fluorescent images of HEK-293 cells obtained after dosing NES-deca-AuNPs with purposely synthesized fluorescent marker show green grains throughout the whole cytoplasm.

Transparency Document

The Transparency document associated with this article can be found, in the online version.

Appendix A. Supplementary data

Supplementary data to this article can be found online at http://dx.doi.org/10.1016/j.bbagen.2015.07.011.

References

[1] M. Ethirajan, Y. Chen, P. Joshi, R.K. Pandey, The role of porphyrin chemistry in tumor imaging and photodynamic therapy, Chem. Soc. Rev. 40 (2011) 340–362.
[2] M. Camerin, M. Magaraggia, M. Soncin, G. Jori, M. Moreno, I. Chambrier, M.J. Cook, D.A. Russell, The *in vivo* efficacy of phthalocyanine–nanoparticle conjugates for the photodynamic therapy of amelanotic melanoma, Eur. J. Cancer 46 (2010) 1910–1918.
[3] R. Bonnett, Photosensitizers of the porphyrin and phthalocyanine series for photodynamic therapy, Chem. Soc. Rev. 24 (1995) 19–33.
[4] L. Marmo Moreira, F. Vieira dos Santos, J. Pereira Lyon, M. Maftoum-Costa, C. Pacheco-Soares, N. Soares da Silva, Porphyrins and phthalocyanines as photosensitizers, Aust. J. Chem. 61 (10) (2008) 741–754.
[5] R.R. Allison, C.H. Sibata, Oncologic photodynamic therapy photosensitizers:a clinical review, Photodiagn. Photodyn. Ther. 7 (2010) 61–75.
[6] Y. Cheng, A.C. Samia, J.D. Meyers, I. Panagopoulos, B. Fei, C. Burda, Highly efficient drug delivery with gold nanoparticle vectors for *in vivo* photodynamic therapy of cancer, J. Am. Chem. Soc. 130 (2008) 10643–10647.
[7] M.E. Wieder, D.C. Hone, M.J. Cook, M.M. Handsley, J. Gavrilovic, D.A. Russell, Intracellular photodynamic therapy with photosensitizer-nanoparticle conjugates: cancer therapy using a 'Trojan horse', Photochem. Photobiol. Sci. 5 (2006) 727–734.
[8] J.R. Casey, S. Grinstein, J. Orlowski, Sensors and regulators of intracellular pH, Nat. Rev. Mol. Cell Biol. 11 (2010) 50–61.
[9] S.T. Whitten, E.B. Garcia-Moreno, V.J. Hilser, Local conformational fluctuations can modulate the coupling between proton binding and global structural transitions in proteins, Proc. Natl. Acad. Sci. U. S. A. 102 (2005) 4282–4287.
[10] S.W. Englander, L. Mayne, M.M.G.Q. Krishna, Protein folding and misfolding: mechanism and principles, Rev. Biophys. 40 (4) (2007) 287–326.
[11] C.W. Bourque, Central mechanisms of osmosensation and systemic osmoregulation, Nat. Rev. Neurosci. 9 (7) (2008) 519–531.
[12] R.D. Vaughan-Jones Spitzer, K.W.P. Swietach, Intracellular pH regulation in heart, J. Mol. Cell. Cardiol. 46 (3) (2009) 318–331.
[13] M. Obara, M. Szeliga, J. Albrecht, Regulation of pH in the mammalian central nervous system under normal and pathological conditions: facts and hypotheses, Neurochem. Int. 52 (6) (2008) 905–919.
[14] J. Pouyssegur, C. Sardet, A. Franchi, G. L'Allemain, S. Paris, A specific mutation abolishing Na^+/H^+ antiport activity in hamster fibroblasts precludes growth at neutral and acidic pH, Proc. Natl. Acad. Sci. U. S. A. 81 (1984) 4833–4837.
[15] M. Thangaraju, K. Sharma, D. Liu, S.H. Shen, C.B. Srikant, Interdependent regulation of intracellular acidification and SHP-1 in apoptosis, Cancer Res. 59 (1999) 1649–1654.
[16] G.C.R. Ellis-Davies, Caged compounds: photorelease technology for control of cellular chemistry and physiology, Nat. Methods 4 (8) (2007) 619–628.
[17] M. Carbone, T. Zlateva, L. Quaroni, Monitoring and manipulation of the pH of single cells using infrared spectromicroscopy and a molecular switch, Biochim. Biophys. Acta Gen. Subj. 1830 (4) (2013) 2989–2993.
[18] G. Sabbatella, S. Antonaroli, M. Diociaiuti, A. Nucara, M. Carbone, Synthesis of proton caged disulphide compounds for gold nanoparticle functionalization, New J. Chem. 39 (2015) 2489–2496.
[19] M. Falk, A.G. Miller, Infrared spectrum of carbon dioxide in aqueous solution, Vib. Spectrosc. 4 (1) (1992) 105–108.
[20] K.K. Sandhu, C.M. McIntosh, J.M. Simard, S.W. Smith, V.M. Rotello, Gold nanoparticle-mediated transfection of mammalian cells, Bioconjug. Chem. 131 (1) (2002) 3–6.
[21] C.M. Wood, P. Pärt, Intracellular pH regulation and buffer capacity in CO_2/HCO_3^- buffered media in cultured epithelial cells from rainbow trout gills, J. Comp. Physiol. B. 170 (3) (2000) 175–184.